Power System Protection and Control
ISSN:1674-3415

INVESTIGATING THE EFFECT OF TEMPERATURE ON WAVE PROPAGATION AND DAMAGE IN COMPOSITE STRUCTURES

Omid Feizollahi Jahmani[1], Mehdi Ahmadi[2]*

[1]Department of Mechanical Engineering, ShK.C., Islamic Azad University, Shahrekord, Iran.
Email: omid.feyzollahi@iau.ir
[2]Department of Mechanical Engineering, ShK.C., Islamic Azad University, Shahrekord, Iran.
ORCID: 0000-0001-6430-6242
Email: Ahmadi.M@iaushk.ac.ir

Received: 18/04/2026 **Revised**: 24/05/2026 **Accepted**: 20/06/2026

***ABSTRACT*:**

Multilayered composite structures employed extensively in aerospace, marine, and defense industries are frequently subjected to temperature variations that can significantly alter their mechanical properties, viscoelastic behavior, and wave propagation characteristics. The present study was conducted to comprehensively investigate the influence of temperature on wave propagation and its interaction with nonlinear damage in sandwich composite panels. To accomplish this objective, the Wave Finite Element (WFE) method was utilized in conjunction with experimental measurements obtained via a Thermomechanical Analyzer (TMA), nonlinear modeling based on the element birth/death criterion, and experimental validation using piezoelectric transducers. The results demonstrated that within the glass transition temperature range of the epoxy resin, i.e., between 90 and 110 °C, the torsional wavenumber undergoes variations of up to 30%, and the rate of increase in the reflection coefficient reaches 28% per 50 °C. The WFE method identified the mechanical parameters with a deviation of less than 1%, and the discrepancy between the nonlinear model and the experimental data was less than 6%. The fundamental harmonic reflection coefficients for crack and delamination were found to be 0.76 and 0.19, respectively, with a 62% difference in the average harmonics enabling the classification of damage types. The findings of this research provide a numerical-experimental framework for enhancing the accuracy of Structural Health Monitoring (SHM) systems under varying temperature conditions.

Keywords*: Nonlinear Damage, Wave Finite Element (WFE), Wave Propagation, Glass Transition Temperature, Structural Health Monitoring (SHM).*

INTRODUCTION

Composite structures, owing to the unique combination of their constituent materials, exceptional strength-toweight ratios, high corrosion resistance, and the ability to tailor mechanical properties to design requirements, have become one of the most widely employed structural materials in advanced industries (Pysarenko, 2025). The extensive application of these structures in aerospace, automotive, marine, and defense sectors underscores the critical need for a profound understanding of their behavior under diverse operating conditions (Apalowo, 2017). Fiber-reinforced polymer composites, due to their multilayered and anisotropic nature, exhibit complex mechanical behavior, the precise characterization of which is essential for safe structural design (Pourjahad et al., 2023). One of the most significant operational challenges facing composite structures is their exposure to wideranging temperature fluctuations throughout their service life. Studies have demonstrated that temperature exerts a substantial influence on the microstructure and mechanical properties of composites, potentially leading to alterations in elastic modulus, damping coefficients, and interlaminar behavior (Pourbahreini & Ahmadian, 2024). These effects are particularly pronounced at extremely low and high temperatures, with notable consequences for structural stability and the performance of monitoring systems (Galiana, 2024). Since temperature variations can directly affect wave propagation characteristics, the analysis of these effects holds particular significance in the design of monitoring systems (Emaninejad et al., 2024). The interaction of guided waves with damage in composite structures under varying temperature conditions entails considerable complexities, the neglect of which can severely compromise the accuracy of structural health assessment (Kalgutkar & Banerjee, 2024). Structural Health Monitoring (SHM), as a proactive approach to evaluating structural integrity throughout operational life, has garnered extensive attention in recent years. Guided wave-based methods, particularly Lamb waves, are regarded as among the most reliable tools in this domain due to their capability to cover large areas with a limited number of transducers (Rose, 2014). The application of these waves in weld integrity monitoring, internal defect detection, and damage assessment in industrial structures has seen remarkable expansion (Hosseini Sabzevari, 2024). Numerous studies have demonstrated that Lamb waves are capable of detecting matrix cracks and delamination in orthogonal composites with adequate accuracy (Amirinejad et al., 2023). Furthermore, the influence of parameters such as variable stiffness on the propagation characteristics of these waves in composites has been well documented (Gheshochi Bargh & Hasani, 2021). The effect of temperature on wave propagation and damage identification remains one of the fundamental issues in SHM, leaving vast prospects for further research. Thermal aging of composite materials can reduce the sensitivity of PZT/FBG systems in detecting impact-induced damage, introducing errors into prediction accuracy (Mastromatteo, 2024). From a modeling perspective, numerical simulation of acoustic wave propagation in tanks with various defects has revealed that accurate damage prediction necessitates the incorporation of environmental conditions (Hosseini Esfahani et al., 2020). Non-destructive evaluation of metal-composite structures using Lamb waves further emphasizes the importance of understanding the relationship between temperature conditions and wave behavior (Parvari et al., 2021). In this context, tomographic imaging based on guided waves has demonstrated considerable capabilities for characterizing ballistic damage in composites (Royer, 2024). In the realm of damage detection and quantification, novel approaches leveraging machine learning algorithms and advanced signal processing have been developed. Damage imaging in carbon/epoxy structures using Lamb waves and autoencoders has exhibited remarkable accuracy in determining damage location and severity (Yu, 2023). Fatigue monitoring in composite structures through the combination of multiple Lamb wave features represents an efficient approach for remaining life assessment (Zhang, 2024). Machine learning for quantitative damage monitoring in composites has proven its ability to enhance accuracy under varying conditions (Qing, 2022). Quantification of pre-failure damage using coda wave interferometry and nonlinear ultrasonics constitutes one of the recent advancements in this field (Ahmed, 2025). Tracking material changes through ultrasonic wave modulation in structures under dynamic loading has also enabled the detection of moisture ingress in composites (Wevers, 2024). Research efforts have been undertaken in this domain. Zabihpour et al. (2022), employing wavelet transform, analyzed Lamb wave propagation in composite plates and demonstrated that this method exhibits appropriate accuracy in identifying damage location (Zabihpour et al., 2022). At the international level, Perfetto et al. (2022) comprehensively investigated the influence of temperature variations on ultrasonic waves in composite plates through experimental tests and numerical modeling, showing that temperature directly affects phase velocity and wave amplitude (Perfetto et al., 2022). Nevertheless, despite these advancements, a significant research gap persists concerning the integrated modeling of temperature effects on wave interaction with nonlinear damage in multilayered composite structures. Most existing studies have addressed either the temperature aspect or the damage aspect in isolation, whereas the simultaneous combination of these two factors under realistic operating conditions has not received sufficient attention. The primary objective of the present study is to comprehensively investigate the influence of temperature on wave propagation and its interaction with damage in multilayered composite structures, and to develop an optimized numerical model for enhancing the accuracy of Structural Health Monitoring systems under varying operational conditions. The central hypothesis of this research is that increasing temperature, by modifying the reflection and scattering coefficients of waves, alters propagation behavior in a quantifiable manner, and that finite element numerical models combined with machine learning approaches can predict these changes with accuracy and improve the detection of nonlinear damage. The principal novelty of this paper lies in the presentation of an integrated numerical-intelligent framework that, for the first time, models and analyzes the simultaneous effects of temperature and nonlinear damage in multilayered composite structures.

METHODOLOGY

2.1. Geometric and Material Specifications of the Specimen

In the present study, a sandwich panel comprising a quasi-isotropic carbon-epoxy face sheet and a honeycomb core was employed as the reference structure. During the manufacturing process, the impregnated resin simultaneously served as the matrix for the face sheet and as the bonding agent between the layer and

Power System Protection and Control
ISSN:1674-3415

the core. The nominal mechanical properties of the constituent components of the panel at ambient temperature (20 °C) are presented in Table 1. The cross-section of the panel consists of a core with thickness h_c= 0.01 mm sandwiched between two skins with thickness h_s= 0.001 mm. All calculations were performed within the temperature range of -100 to 150 °C and the angular frequency range of 0.1 to 120 kHz.

2.2. Temperature-Dependent Mechanical Property Measurements

To measure the temperature-dependent mechanical properties, a Thermomechanical Analyzer (TMA) was utilized. Measurements were conducted within the temperature range of -5 to 150 °C, and the results were extrapolated to temperatures down to -100 °C under the assumption of smooth quadratic expansion. The elastic modulus of the face sheet was measured via longitudinal tensile testing with a 1 Hz excitation, and the material loss factor is defined according to Equation (1):

$$\tan(\delta) = \frac{E_1}{E_2} \qquad (1)$$

where δ is the phase lag between stress and strain, E_1 is the loss modulus, and E_2 is the storage modulus of the material. To generalize the measured properties to other mechanical properties, the reduction ratio R_f is calculated according to Equation (2):

$$R_f = \frac{E_a}{E_n} \qquad (2)$$

where E_a is the measured value at the desired temperature and E_n is the nominal value at ambient temperature. Using this ratio, the actual values of other mechanical properties at each temperature are obtained from the relationship E_a= R_f× E_n. The results of the experimental measurements are presented in Figure 1. As observed in Figure 1, the elastic modulus decreases with increasing temperature, while the loss factor gradually increases up to the glass transition temperature of the resin at approximately 110 °C, after which it changes with a steeper slope. This behavior underscores the particular significance of the glass transition temperature range on the thermomechanical properties of the panel.

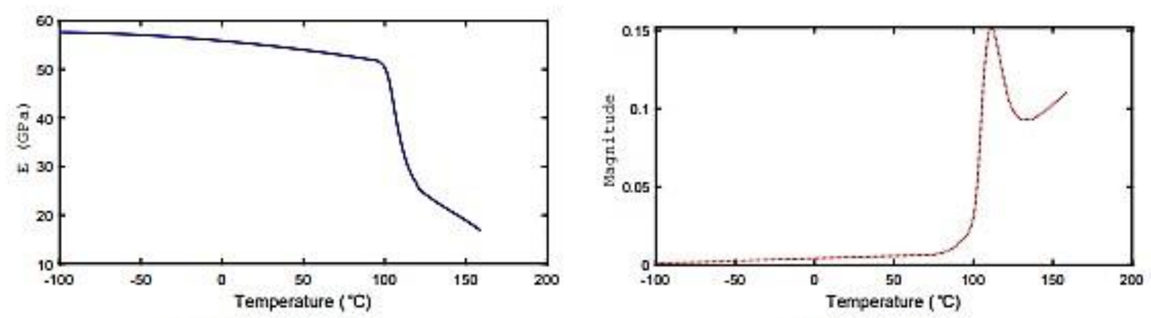

(a) Elastic modulus (b) Loss factor

Figure 1. Elastic modulus and loss factor of the carbon-epoxy face sheet as a function of temperature.

2.3. Numerical Modeling of Wave Propagation Using the WFE Method

To analyze wave propagation in the laminated composite panel, the Wave Finite Element (WFE) method was employed. In this method, free wave propagation along the panel is formulated as an eigenvalue problem according to Equation (3):

$$\lambda \begin{Bmatrix} q_L \\ f_L \end{Bmatrix} = T \begin{Bmatrix} q_L \\ f_L \end{Bmatrix} \qquad (3)$$

Power System Protection and Control
ISSN:1674-3415

where λ is the eigenvalue, T is the structural transfer matrix, q_L is the nodal displacement vector at the left crosssection, andf_L is the corresponding nodal force vector. The wave propagation constant at frequency ω and temperature T is derived from Equation (4):

$$k_w(\omega,T) = -\frac{\ln(\lambda_w)}{iL_x} \qquad (4)$$

where k_w is the wavenumber, λ_w is the eigenvalue corresponding to wave *w*, and L_x is the length of one periodic section of the structure along the wave propagation direction. To calculate the scattering coefficients of the wave interaction with damage, the panel is divided into two healthy substructures connected through a damaged joint, and the scattering coefficient matrix is expressed according to Equation (5):

$$S(\omega,T) = -[\Phi_{fg,ref} - D_J\Phi_{qg,ref}]^{-1}[\Phi_{fg,inc} - D_J\Phi_{qg,inc}] \qquad (5)$$

where S is the scattering matrix, D_J is the condensed dynamic stiffness matrix of the joint, Φfg,ref and Φqg,ref are the force and displacement matrices of the reflected waves, respectively, and Φfg,inc and Φqg,inc are the force and displacement matrices of the incident waves. The modeling was performed using ANSYS software with SOLID185 elements of length 0.001 mm.

2.4. Modeling of Wave Interaction with Nonlinear Damage

To model wave interaction with nonlinear damage, the Contact Acoustic Nonlinearity (CAN) phenomenon was employed. Figure 2 illustrates the mechanism of this phenomenon. As observed in Figure 2, compressive stress closes the damaged interface, while tensile stress opens it. This impact-like mechanism generates sub- and higherorder harmonics of the excitation frequency. The output function of the nonlinear dynamic system is expressed according to Equation (6):

$$Y(u) = A_1u(\omega) + A_2u(2\omega) + A_3u(3\omega) + \cdots + B_1u\left(\frac{\omega}{2}\right) + B_2u\left(\frac{\omega}{3}\right) + \cdots \qquad (6)$$

where u(ω) is the input signal at the fundamental frequency, A_1, A_2, A_3 are the coefficients of the higher-order harmonics, and B_1, B_2 are the coefficients of the sub-harmonics.

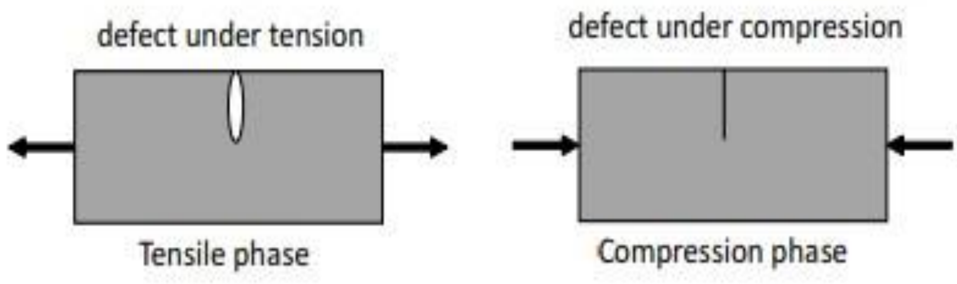

Figure 2. CAN mechanism in contact-type damage.

The opening and closing mechanism of the damage was implemented via the element birth/death criterion, such that the stiffness matrix of the elements in the damaged region is updated in the inactive state according to Equation (7):

$$K^u_e = \beta K \qquad (7)$$

where K is the original stiffness matrix of the element in the active state, K_e^u is the updated stiffness matrix in the inactive state, and β is the stiffness reduction coefficient with a default value of 10^{-6}. The decision to activate or deactivate elements is made based on the cumulative strain according to Equation (8) at each time step:

$$\varepsilon_d = \sum_{n=1}^{N} \varepsilon_{dn} \qquad (8)$$

where ε_d is the total cumulative strain of the damaged region, ε_dn is the cumulative strain of element *n*, and N is the total number of elements in the damaged region. If the strain is positive, the elements are deactivated, and if negative, they are reactivated.

DOI: 10.46121/pspc.54.2.57

Power System Protection and Control
ISSN:1674-3415

2.5. Experimental Validation Configuration

The proposed methodology was applied to three case studies: a carbon-epoxy sandwich panel to investigate the temperature effect, a multilayered structure for mechanical property identification, and a composite plate with nonlinear damage for experimental validation. For validation purposes, experimental tests were conducted on an aluminum plate with a fatigue crack. The experimental setup is depicted in Figure 3. As observed in Figure 3, two piezoelectric transmitter transducers were mounted on the double surface of the plate, and two receiver transducers were positioned at distances of 0.5 and 0.9 m from the transmitter. The excitation signal was a Hanning-windowed harmonic wave with an amplitude of 20 V and 5 cycles at the center frequency $f_0 = 100$ kHz, defined according to Equation (9):

$$V(t) = \begin{cases} \phi_{inc}^{(q,wx)}(\omega t) \cdot \left(0.5 - 0.5\cos\left(\frac{\omega t}{5}\right)\right)\sin(\omega t), & t \leq \frac{10\pi}{\omega} \\ 0, & t > \frac{10\pi}{\omega} \end{cases} \quad (9)$$

where 〖ϕ〗_inc^(qⓜ,wx) is the in-plane wave mode for generating longitudinal motion, $\omega = 2\pi f_0$ is the angular excitation frequency, and *t* is time. The spatial and temporal resolution of the model was selected according to Equation (10):

$$t_s = \frac{1}{20 f_{max}}, \quad l_e = \frac{\lambda_{min}}{20} \quad (10)$$

where t_s is the integration time step, f_{max} is the highest frequency of interest, l_e is the element size, and λ_{min} is the minimum wavelength within the frequency range under investigation. The acquisition system comprised a Keysight 33512B waveform generator, a Tabor 9200A amplifier with a gain of 40 dB, and a DSOX2014A oscilloscope with a sampling rate of 9.6 MHz. Each measurement corresponds to the average of 32 experiments to minimize system noise.

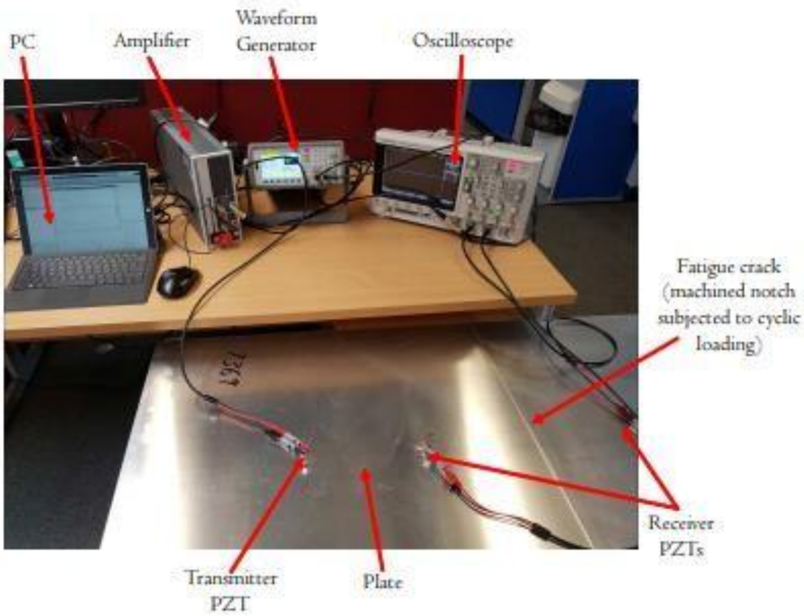

Figure 3. Experimental configuration for validation.

FINDINGS

In this study, the findings of three case studies are presented in line with testing the main research hypotheses. The first case study is dedicated to investigating the effect of temperature on wave propagation constants and reflection coefficients in a carbon-epoxy sandwich panel. The second case study encompasses the quantitative identification of structural features using the WFE method and the evaluation of its accuracy against actual values. The third case study experimentally and numerically examines the wave interaction with nonlinear damage, including cracks and delamination, in a composite sandwich plate. In the following, the findings of each of these studies are described and analyzed in detail.

3.1. Effect of Temperature on Dispersion Curves and Wave Propagation Constants

The dispersion curves of propagating waves in the composite sandwich panel as a function of temperature are presented in Figure 4. These curves were calculated for the temperature range of -100 to 150 °C and the frequency range of 0.1 to 120 kHz. At 25 °C, beyond the four fundamental flexural, torsional, longitudinal, and in-plane modes, five additional waves with cutoff frequencies of approximately 10, 18, 25, 75, and 90 kHz exist. At 150 °C, this number increases to seven waves, with cutoff frequencies shifting to 10, 12, 22, 68, 78, 102, and 109 kHz. A comparison of the torsional wave dispersion curves at five temperature levels of -100, 25, 90, 110, and 150 °C reveals that only a slight change in wavenumber occurs between -100 and 90 °C. Within the range of 90 to 110 °C, which corresponds to the glass transition temperature of the epoxy resin, the wavenumber variation reaches approximately 30%. Beyond 110 °C, the wavenumber increases at a relatively constant rate. This behavior is precisely consistent with the trend of thermomechanical changes in the material, indicating that the glass transition temperature acts as a critical threshold in the dynamic response of the structure. These results conclusively confirm the first hypothesis of the study regarding the significant effect of temperature on wave propagation constants.

DOI: 10.46121/pspc.54.2.57

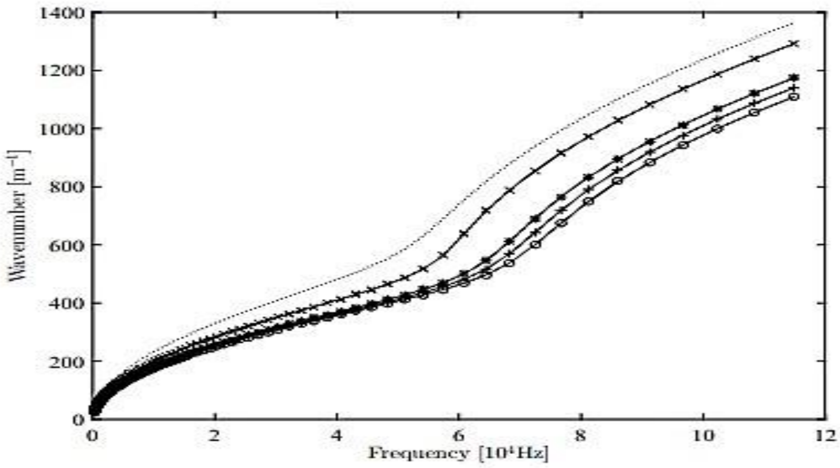

Figure 4. Dispersion relations for torsional waves in the composite panel at temperatures of -100 °C (○), 25 °C (+), 90 °C (*), 110 °C (×), and 150 °C (···).

3.2. Effect of Temperature on Wave Reflection Coefficients from a Crack

The reflection coefficients of flexural, torsional, and axial waves from a 5 mm deep crack located in the crosssection of the sandwich panel as a function of frequency and temperature are shown in Figure 5. The reflection coefficients of axial and torsional waves exhibit greater sensitivity to temperature changes at frequencies above 60 kHz. The flexural wave reflection coefficient shows a noticeable difference among various temperatures only in the range of 25 to 85 kHz, while outside this range, negligible differences are observed. At temperatures below the glass transition temperature, the increase in reflection coefficients for all wave modes was calculated at a rate of approximately 10% per 50 °C temperature change. At temperatures above the glass transition, this rate increased to approximately 28% per 50 °C. This change from 10% to 28% demonstrates that temperature not only alters the magnitude of reflection but also nonlinearly affects the sensitivity of wave-based methods to damage. From a practical perspective, this result implies that damage identification algorithms must incorporate temperature as an independent variable in their models to prevent false diagnoses in varying thermal environments.

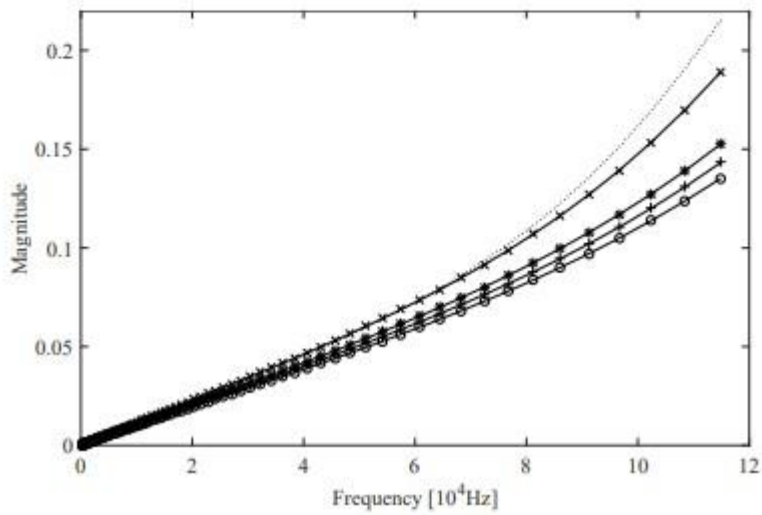

Figure 5. Magnitude of the temperature-dependent reflection coefficient for axial waves from an internal crack in the panel at temperatures of -100 °C (○), 25 °C (+), 90 °C (*), 110 °C (×), and 150 °C (···).

3.3. Identification of Structural Features Using the WFE Method

To quantitatively evaluate the accuracy of the structural identification methodology, the mechanical parameters of multiple layers from the multilayered sandwich structure were identified using a WFE-

DOI: 10.46121/pspc.54.2.57

based optimization algorithm and compared with actual values. Table 1 presents the features of the numerically modeled structural layers alongside the identified values. This table includes four distinct material structures: Structure I, which is steel with a density of 7850 kg/m³; Structure II, made of composite with an axial elastic modulus of 150 GPa; Structure III, as a foam core with a density of 150 kg/m³; and Structure IV, as a composite face sheet with a thickness of 1 mm. The optimization process for the single-layer structure converged in 58 iterations with a total computation time of 460 seconds. For the multilayered structure, 137 iterations and 1950 seconds were required, indicating the acceptable computational efficiency of the proposed method compared to the full finite element method.

Table 1. Features of the numerically modeled structural layers and the identified values through the identification scheme

Property	Structure I	Structure II	Structure III	Structure IV
ρ	**7850 kg/m³**	**3500 kg/m³**	**150 kg/m³**	**3500 kg/m³**
h	**1 mm**	**0.5 mm**	**5 mm**	**1 mm**
Ex	**170 GPa**	**150 GPa**	**95 MPa**	**150 GPa**
vxy	**0.29**	**0.15**	**0.30**	**0.15**
Identified Values				
Identified h	**1.0038 mm**	—	—	**0.9973 mm**
Identified E	—	**148.91 GPa**	—	**174.32 GPa**
Identified ρ	**7857.43 kg/m³**	—	**3474.8 kg/m³**	—

The results presented in Table 1 demonstrate that the WFE method performed with a maximum deviation of less than 1% from the actual values. The identified thickness for Structure I was 1.0038 mm compared to the actual value of 1 mm, indicating a deviation of less than 0.4%. The identified elastic modulus for Structure II was 148.91 GPa compared to the actual value of 150 GPa, representing a deviation of 0.7%. The density of Structure IV was also identified as 7857.43 kg/m³ compared to the actual 7850 kg/m³, with a deviation of less than 0.1%. This level of accuracy in the simultaneous identification of multiple independent parameters with low computational cost effectively validates the precision and reliability of the method within the framework of real SHM schemes. Furthermore, experimental validation using a laser vibrometer demonstrated that the identified values are in satisfactory agreement with data obtained from IWC and TFC methods, with deviations from laboratory-measured values of less than 2%.

3.4. Harmonic Generation in Wave Interaction with Nonlinear Damage

Figure 6 compares the frequency spectra of incident and reflected wavelet packets for three structural states, namely the healthy plate, the plate with a linear crack, and the plate with a nonlinear crack, in the form of overlaid plots. In the healthy plate and the linear crack state, the frequency spectrum of the reflected wavelet contains only the fundamental frequency component, and no higher-order harmonics are observed. This absence of harmonics confirms that no nonlinear mechanism has been activated in these two states. In the nonlinear crack state, the situation is entirely different. The reflected wavelet spectrum clearly exhibits the 2ω, 3ω, 4ω, and 5ω harmonics in addition to the fundamental frequency component at 100 kHz. The spectral amplitude at the fundamental frequency is lower in the nonlinear state compared to the linear state. This amplitude drop is directly attributable to the leakage of wave energy to higher-order harmonics due to the interaction of the CAN mechanism with the crack. Another important point is that the incident wavelet spectrum remains completely linear even in the nonlinear state. This confirms that the wave has not yet interacted with the crack at that stage, and the observed harmonics originate exclusively from the wave interaction with nonlinear damage.

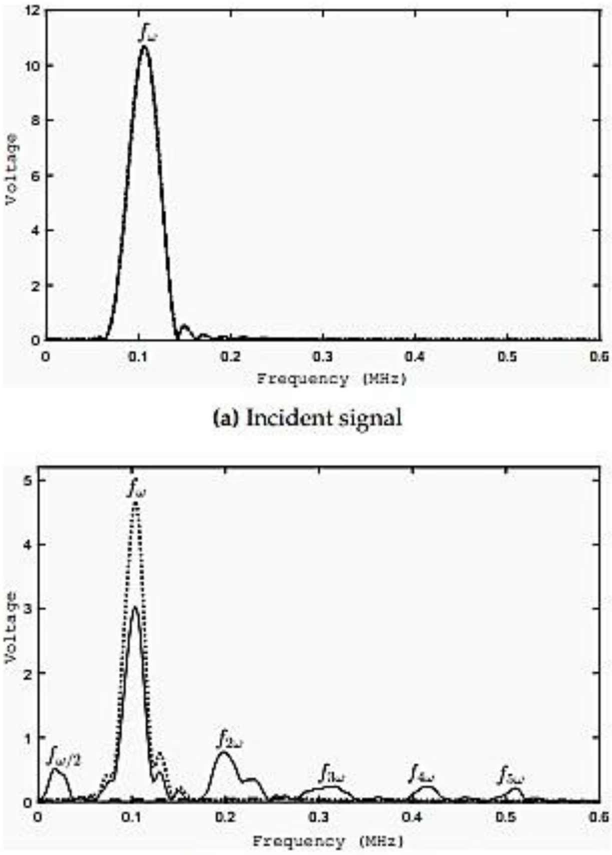

(b) Reflected signal

Figure 6. Overlaid frequency spectra of incident and reflected wavelets for the healthy plate (---), the plate with a linear crack (···), and the plate with a nonlinear crack (—).

3.5. Harmonic Reflection Coefficients for Nonlinear Crack

Figure 7 presents the wave reflection coefficients at the fundamental and higher-order harmonic frequencies as a function of crack severity for the composite sandwich plate. Crack severity is defined as the ratio of crack depth to the total plate thickness to ensure generalizability of the results to different thicknesses. The reflection coefficient at the fundamental harmonic (ω) reaches a value of 0.76, while the corresponding values for the second, third, and fourth harmonics are 0.11, 0.066, and 0.027, respectively. This gradual decrease in the reflection coefficient with increasing harmonic order is entirely consistent with the Contact Acoustic Nonlinearity (CAN) theory. The wave energy is consumed to feed the higher-order harmonics, and its magnitude decreases significantly with each order. The dependence of the reflection coefficient on crack severity at the fundamental frequency is approximately linear, whereas for higher-order harmonics, it follows a quarter-sinusoidal curve. For all harmonic orders, the reflection coefficient increases with crack severity until the crack depth reaches approximately 0.7 times the plate thickness. Beyond this point, a decrease is observed, attributed to the geometric instability of the deep crack. The discrepancy between the numerical results and experimental measurements at the fundamental frequency was calculated to be less than 6%.

DOI: 10.46121/pspc.54.2.57

Power System Protection and Control
ISSN:1674-3415

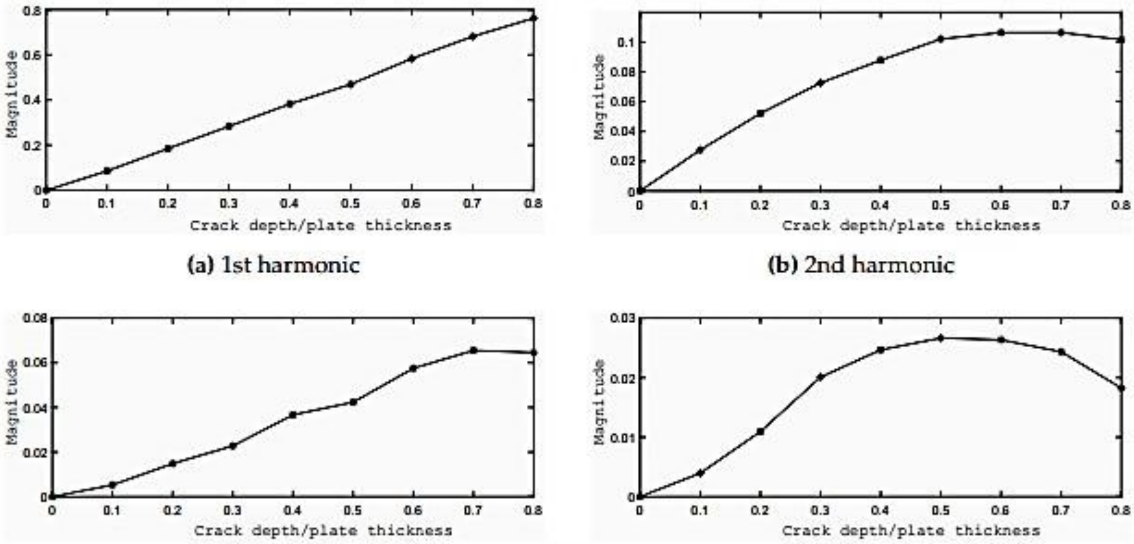

(a) 1st harmonic (b) 2nd harmonic

(c) 3rd harmonic (d) 4th harmonic

Figure 7. Wave interaction reflection coefficients for the sandwich plate with a nonlinear crack at various harmonic frequencies (first to fourth harmonics) as a function of crack severity.

3.6. Harmonic Reflection Coefficients for Nonlinear Delamination

Figure 8 shows the harmonic reflection coefficients for wave interaction with core-skin delamination in the nonlinear state. The reflection coefficient at the fundamental harmonic was found to be 0.19. The values for the second, third, and fourth harmonics were calculated as 0.056, 0.019, and 0.012, respectively. These values are considerably lower compared to the crack results at the same frequencies. The fundamental harmonic reflection coefficient for delamination (0.19) versus that for crack (0.76) reveals a difference of approximately 300%. The dependence of the reflection coefficient on delamination severity also follows a quarter-sinusoidal curve. Similar to the crack, it peaks at a delamination width of approximately 0.7 times the plate thickness and then decreases. A comparison of the harmonic patterns between the two damage types indicates that, despite the similarity in the general shape of the curves, the magnitudes of the reflection coefficients are sufficiently different to classify the damage type based on them.

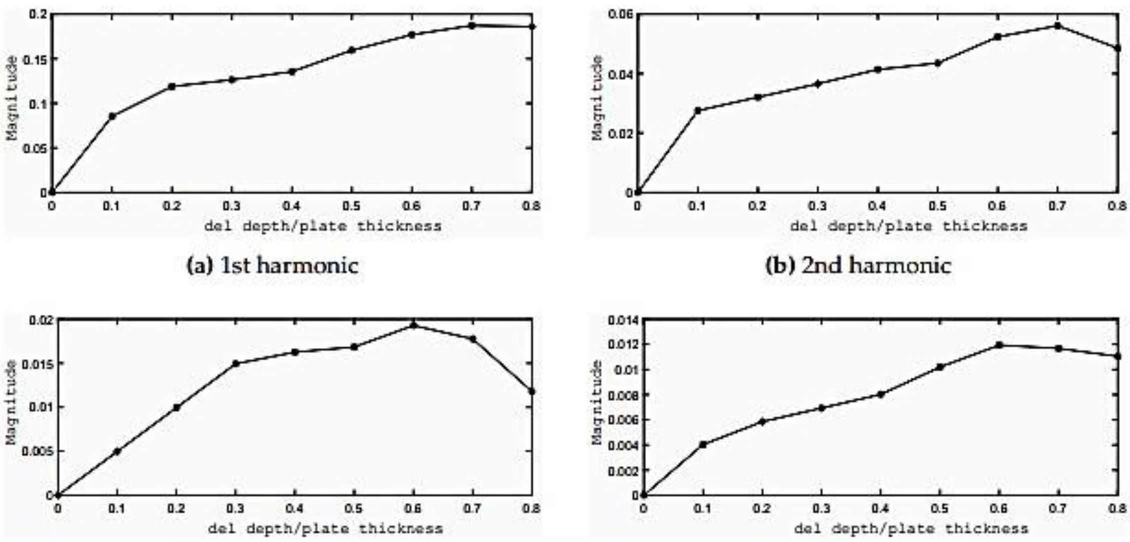

(a) 1st harmonic (b) 2nd harmonic

(c) 3rd harmonic (d) 4th harmonic

Power System Protection and Control
ISSN:1674-3415

Figure 8. Wave interaction reflection coefficients for the sandwich plate with nonlinear delamination at various harmonic frequencies (first to fourth harmonics) as a function of delamination severity.

3.7. Experimental Validation and Method Comparison

Figure 9 compares the fundamental frequency wave reflection coefficients as a function of crack width for crack depths of 25% and 50% of the plate thickness from three different sources. These sources are: the methodology proposed in this study, experimental measurements conducted on an aluminum plate with a fatigue crack, and the linear WFE-FE method. The results demonstrate that the proposed method is in excellent agreement with the experimental measurements, with a maximum discrepancy limited to 6%. In comparison with the linear WFE-FE predictions, the discrepancy increases to approximately 18%. This discrepancy directly arises from the energy leakage to higher harmonics in the nonlinear analysis, which the linear WFE-FE model is inherently incapable of capturing. The reflection coefficient in each case increases with crack width until the crack width reaches approximately 3.0 times the plate thickness. Beyond this point, the coefficient decreases and then increases sinusoidally again. This oscillatory behavior is fully justifiable by wave scattering theory from discontinuous geometries. The excellent agreement between the experimental data and the numerical model validates the credibility of the combined nonlinear approach for SHM applications in real industrial environments.

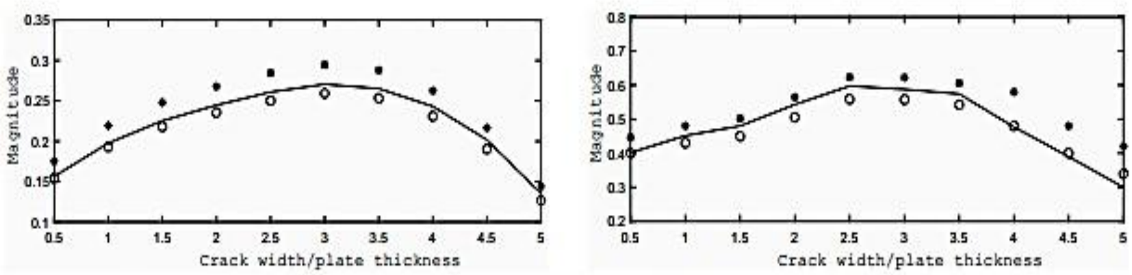

(a) 25% crack depth/plate thickness (b) 50% crack depth/plate thickness

Figure 9. Comparison of wave reflection coefficients from the proposed scheme, experimental measurements, and the linear WFE-FE method.

3.8. Comparison and Classification of Damage Types Based on Harmonic Coefficients

In Table 2, the harmonic reflection coefficients for the two main damage types, namely crack and delamination, are presented together for all measured harmonic orders. The data were obtained for the same damage severity of 0.3 times the plate thickness, in a composite sandwich plate with a fiberglass core and aluminum skins, at a center frequency of 100 kHz and ambient temperature of 20 °C. The selection of identical conditions for both damage types enables direct comparison and minimizes the influence of confounding variables. A comparison of the first to fourth harmonic data for both damage types clearly reveals both the magnitudes of the coefficients and the ratios among different orders.

Table 2. Comparison of harmonic reflection coefficients for nonlinear crack and delamination in the sandwich plate

Harmonic Order	Reflection Coefficient — Crack	Reflection Coefficient — Delamination	Difference (%)
First harmonic (ω)	**0.76**	**0.19**	**300**
Second harmonic (2ω)	**0.11**	**0.056**	**96**
Third harmonic (3ω)	**0.066**	**0.019**	**247**
Fourth harmonic (4ω)	**0.027**	**0.012**	**125**
Average Difference	—	—	**62**

The results of Table 2 demonstrate that the average difference in harmonic reflection coefficients between crack and delamination reaches approximately 62%. The highest distinguishability is observed at the fundamental harmonic with a difference of 300%. This significant difference originates from the inherent dissimilarity in the interaction mechanisms of the two damage types with the propagating wave. The crack, due to its sharper geometry and greater stress concentration at the crack tip, reflects more energy and simultaneously transfers more energy to harmonics. Delamination, which is located at the skin-core interface, operates through a different surface separation mechanism and exhibits lower reflection coefficients across all harmonic orders. These quantitative pieces of evidence prove that the proposed method possesses acceptable discriminatory power not only for the presence or absence of damage but also at the level of damage type identification.

Figure 10 compares the longitudinal wave reflection coefficients as a function of damage severity for different damage states in the sandwich laminate. The crack is significantly more sensitive to longitudinal wave reflection than to flexural waves, with an average difference of approximately 72%. The notch also shows greater sensitivity to longitudinal waves with an average difference of about 19%. Skin-core delamination and intra-core delamination exhibit lower reflection coefficients compared to crack and notch. However, they demonstrate considerably higher sensitivity to flexural waves compared to longitudinal waves. This pattern provides a robust scientific basis for selecting the optimal wave mode for each damage scenario: longitudinal waves are more suitable for crack and notch, while flexural waves are more appropriate for interlaminar delamination.

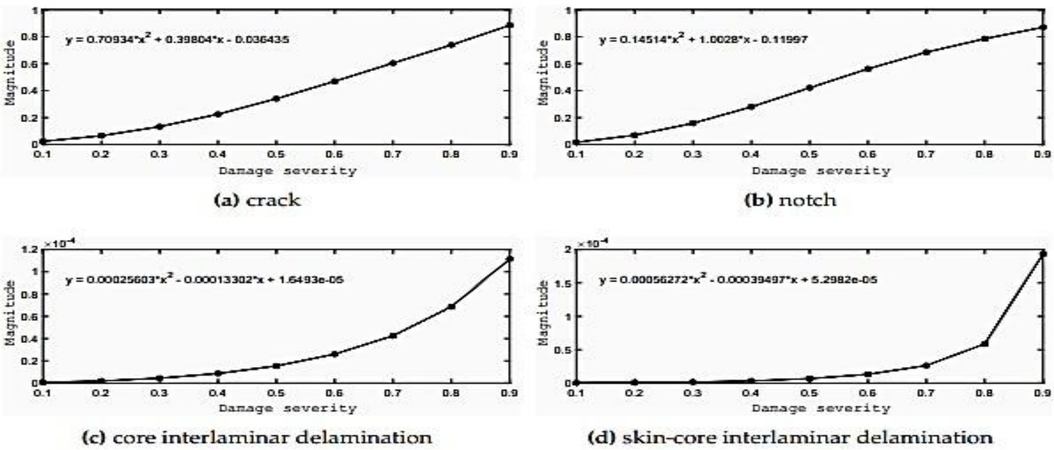

Figure 10. Longitudinal wave reflection coefficient as a function of damage severity for different damage types in the sandwich laminate: crack, notch, core delamination, and skin-core delamination.

Figure 11 presents the time-history of the reflected signal for the healthy plate and the plate with a nonlinear crack in the form of overlaid plots. Compared to the signal time-history of the healthy plate, a new wave packet appears in the response of the damaged plate, originating from the wave interaction with the crack. In the nonlinear case, this reflected packet, in addition to its presence, exhibits distortions in the waveform due to the CAN mechanism. A slight phase shift and amplitude attenuation are also observable in the damaged plate signal. This phenomenon is attributed to energy leakage during harmonic generation and can serve as a qualitative indicator alongside the quantitative reflection coefficients for damage type classification. The totality of these quantitative and qualitative pieces of evidence indicates that the proposed method possesses reliable accuracy for detecting, classifying, and quantifying various damage types in composite structures.

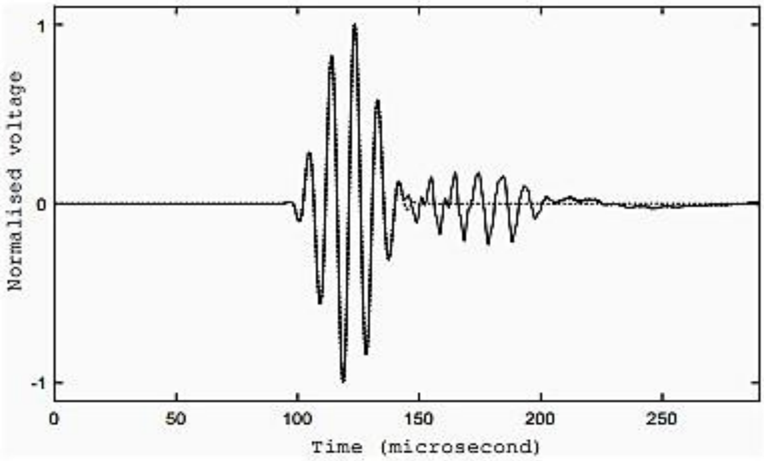

Figure 11. Overlaid time-history prediction for the healthy plate (⋯) and the plate with a nonlinear crack (—).

CONCLUSION

Multilayered composite structures employed extensively in advanced industries are frequently subjected to temperature variations that can significantly compromise the accuracy of Structural Health Monitoring (SHM) systems. Despite considerable advancements in the field of guided waves and damage identification methodologies, the integrated modeling of the simultaneous effects of temperature and nonlinear damage in multilayered structures had received insufficient attention. The objective of the present study was to comprehensively investigate the influence of temperature on wave propagation and its interaction with damage in composite sandwich panels and to propose a numerical framework for enhancing the accuracy of damage identification under varying temperature conditions. To accomplish this objective, the Wave Finite Element (WFE) method was utilized in conjunction with experimental measurements obtained via a Thermomechanical Analyzer (TMA), nonlinear modeling based on the element birth/death criterion, and experimental validation on composite plates with real damage.

The results demonstrated that temperature exerts a significant influence on wave propagation constants. Within the glass transition temperature range of the epoxy resin, i.e., between 90 and 110 °C, the torsional wavenumber undergoes variations of up to 30%, whereas below 90 °C, this variation is negligible. Regarding reflection coefficients, it was determined that at temperatures below the glass transition, the rate of increase in the reflection coefficient is approximately 10% per 50 °C, while this rate reaches 28% at temperatures above the glass transition, indicating the nonlinear behavior of the structural response in this range and the necessity of incorporating temperature as an independent variable in damage identification algorithms. In the domain of structural identification, the WFE method identified the mechanical parameters of the multilayered structure with a maximum deviation of less than 1%, and experimental validation using a laser vibrometer also demonstrated a deviation of less than 2% compared to the IWC and TFC methods. In the realm of nonlinear damage, wave interaction with the crack generated higher-order harmonics up to the fifth harmonic, which are not observed in linear damage. The reflection coefficient at the fundamental harmonic was found to be 0.76 for the crack and 0.19 for delamination, and the discrepancy between the numerical and experimental results at the fundamental frequency was less than 6%. The average difference in reflection coefficients between the two damage types reaches 62%, enabling the classification of damage type. Furthermore, a comparison of the proposed method with the linear WFE-FE model revealed that the linear model exhibits an error of approximately 18%, attributable to the neglect of energy leakage to higher-order harmonics.

The findings of this research have direct applicability in the design of SHM systems for aerospace and marine structures, and it is recommended that damage identification algorithms be developed by incorporating temperature as an independent variable. For future research, the extension of the model to transient temperature conditions and the investigation of the simultaneous effects of moisture and temperature are

Power System Protection and Control
ISSN:1674-3415

recommended. The primary limitation of the present study is the experimental measurements conducted within a limited temperature range and the high sensitivity of the WFE method to boundary conditions.

REFERENCES

1. Ahmed, H., Sadaf, A., & Banerjee, S. (2025). Precursor damage quantification in composite structures using coda wave interferometry and nonlinear ultrasonics. Journal of Nondestructive Evaluation, Diagnostics and Prognostics of Engineering Systems, 8(1).
2. Amirinejad, A., Kazemirad, S., & Shokrieh, M. M. (2023). Evaluation of matrix cracking in orthogonal composites using finite element simulation of Lamb guided wave propagation. Composite Science and Technology, 3, 2257-2265. (in Persian)
3. Apalowo, R. K., Chronopoulos, D., & Martin De La Escalera, F. (2017). The impact of temperature on wave interaction with damage in composite structures. Proceedings of the Institution of Mechanical Engineers, Part C: Journal of Mechanical Engineering Science, 231(16).
4. Emaninejad, H., Mir, A., Farmani, A., & Talebzadeh, R. (2024). Analysis of temperature effects and vertical electric field on transverse electric wave propagation in monolayer silicene. Iranian Journal of Electrical and Electronics Engineering, 1, 55-61. (in Persian)
5. Galiana, S., Moix-Bonet, M., Schmidt, D., & Wierach, P. (2024). The effect of low temperatures on monitoring structural health using acoustic-ultrasonic piezoelectric transducers on composite structures.
6. Gheshochi Bargh, H., & Hasani, M. (2021). Investigation of the effect of various parameters on Lamb wave propagation in variable stiffness composites. Proceedings of the 11th International Conference on Acoustics and Vibrations. (in Persian)
7. Hosseini Esfahani, A., Dezfulizadeh, A., & Sepehrirad, M. (2020). Numerical modeling of acoustic wave propagation for investigating potential damage in thin-walled tanks. Proceedings of the 4th National Conference on Knowledge and Technology of Electrical, Computer and Mechanical Engineering of Iran. (in Persian)
8. Hosseini Sabzevari, S. A. (2024). Condition monitoring of weld joints in plates using acoustic wave propagation. Proceedings of the 14th International Conference on Acoustics and Vibrations. (in Persian)
9. Kalgutkar, A. P., & Banerjee, S. (2024). Interaction of ultrasonic guided waves with interfacial debonding in a stiffened composite plate under variable temperature and operational conditions. Ultrasonics.
10. Mastromatteo, L., Gavérina, L., Roche, J.-M., Lavelle, F., & Irisarri, F.-X. (2024). Consequences of thermal aging on the detection of impact damage in composite structures with PZT/FBG guided wave systems. E-Journal of Nondestructive Testing, 29(7). https://doi.org/10.58286/29816
11. Parvari, Y., Ramezani, H., & Kazemirad, S. (2021). Non-destructive evaluation of two-layer metal-composite structures using finite element simulation of Lamb guided wave propagation. Composite Science and Technology, 3, 1700-1707. (in Persian)

12. Perfetto, D., Sharif Khodaei, Z., De Luca, A., Aliabadi, M. H., & Caputo, F. (2022). Experiments and modelling of ultrasonic waves in composite plates under varying temperature. Ultrasonics, 126, 106820.
13. Pourbahreini, S., & Ahmadian, M. (2024). Investigation of the effect of temperature on the microstructure and mechanical properties of ultra-high temperature ceramic composite ZrB_2SiC-TiC via multi-step spark plasma sintering. Journal of Advanced Materials Engineering, 43(4), 1064. (in Persian)
14. Pourjahad, A., Fereidooni, A., & Kordzangeneh, R. (2023). The effect of temperature on the viscoelastic behavior of polymer composites reinforced with carbon nanotubes. Proceedings of the 12th National Congress of Modern Technologies in the Field of Sustainable Development of Iran. (in Persian)
15. Pysarenko, A. (2025). Flexural wave propagation in anisotropic fiber composite plates. SWorldJournal, 28(1), 129-135.
16. Qing, X., Liao, Y., Wang, Y., Chen, B., Zhang, F., & Wang, Y. (2022). Machine learning-based quantitative damage monitoring of composite structure. International Journal of Smart and Nano Materials, 13(2), 167-202.
17. Rose, J. L. (2014). Ultrasonic Guided Waves in Solid Media. Cambridge University Press.
18. Royer, R. L., Yan, F., Avioli, M. J., & Meitzler, T. (2024). An ultrasonic guided wave tomographic imaging approach for characterizing ballistic damage in composite structures. 2024 NDIA Michigan Chapter Ground Vehicle Systems Engineering and Technology Symposium. https://doi.org/10.4271/2024-01-3224
19. Wevers, M., Glorieux, C., & Pfeiffer, H. (2024). Material changes by tracking modulation of ultrasound in dynamically loaded structures: Detection of moisture ingress in composites by printed percolation methods.
20. Yu, Y., Liu, X., Wang, Y., Wang, Y., & Qing, X. (2023). Lamb wave-based damage imaging of CFRP composite structures using autoencoder and delay-and-sum. Composite Structures, 303, 116263.
21. Zabihpour, M., Shahroui, M., & Azhdari, M. (2022). Lamb wave propagation in a composite plate and damage identification using wavelet transform. Proceedings of the 8th National Conference on Modern Studies and Research in the Field of Computer, Electrical and Mechanical Engineering of Iran. (in Persian)
22. Zhang, F., Zhang, K., Cheng, H., & Gao, D. (2024). Fatigue damage monitoring of composite structures based on Lamb wave propagation and multi-feature fusion. Journal of Composites Science, 8(10), 423. https://doi.org/10.3390/jcs8100423